HHS Public Access

Author manuscript

J Immunol. Author manuscript; available in PMC 2023 February 01.

Published in final edited form as:

J Immunol. 2022 February 01; 208(3): 745–752. doi:10.4049/jimmunol.1901171.

Bone marrow transplantation rescues monocyte recruitment defect and improves cystic fibrosis in mice

Zhichao Fan[*,†,1], **Elise Pitmon**[†,1], **Lai Wen**[*], **Jacqueline Miller**[*], **Erik Ehinger**[*], **Rana Herro**[‡], **Wei Liu**[†], **Ju Chen**[†], **Zbigniew Mikulski**[§], **Douglas J. Conrad**[¶], **Alex Marki**[*], **Marco Orecchioni**[*], **Puja Kumari**[†], **Yanfang Peipei Zhu**[*], **Paola M. Marcovecchio**[*], **Catherine C. Hedrick**[*], **Craig A. Hodges**[‖], **Vijay A. Rathinam**[†], **Kepeng Wang**[†], **Klaus Ley**[*,#]

[*]Division of Inflammation Biology, La Jolla Institute for Immunology, 9420 Athena Circle Drive, La Jolla, California 92037, USA

[†]Department of Immunology, School of Medicine, UConn Health, 263 Farmington Ave, Farmington, Connecticut 06030, USA.

[‡]Division of Immunobiology, Cincinnati Children's Hospital Medical Center, Cincinnati, OH, USA

[§]Microscopy and Histology Core Facility, La Jolla Institute for Immunology, 9420 Athena Circle Drive, La Jolla, California 92037, USA

[¶]Division of Pulmonary, Critical Care and Sleep Medicine, Department of Medicine, University of California San Diego, 9500 Gilman Drive, La Jolla, California 92093, USA

[‖]Department of Genetics and Genome Sciences, Cystic Fibrosis Mouse Models Core, School of Medicine, Case Western Reserve University, 2109 Adelbert Rd, Cleveland, Ohio 44106, USA

[#]Department of Bioengineering, University of California San Diego, 9500 Gilman Drive, La Jolla, California 92093, USA

Abstract

Cystic fibrosis (CF) is an inherited life-threatening disease accompanied by repeated lung infections and multi-organ inflammation that affects tens of thousands of people worldwide. The causative gene, cystic fibrosis transmembrane conductance regulator (CFTR), is mutated in CF patients. CFTR functions in epithelial cells have traditionally been thought to cause the disease symptoms. Recent work has shown an additional defect: monocytes from CF patients show a deficiency in integrin activation and adhesion. Since monocytes play critical roles in

Address correspondence to: Klaus Ley, M.D., La Jolla Institute for Immunology, 9420 Athena Circle Drive, La Jolla, CA 92037. Phone: (858) 752-6661; Fax: (858) 752-6985; klaus@lji.org.

[1]equally contributed

Author Contributions

Z.F. and E.P. contributed equally to this work. Experiments were designed by Z.F. and K.L. Most experiments were performed by Z.F., E.P., L.W. J.M., E.E., R.H., W.L., J.C, A.M., M.O., P.K., and Z.M. Data analysis was performed by Z.F., E.P., L.W., Y.P.Z., and P.M.M. A critical mouse strain was provided by C.A.H. The manuscript was written by K.L., Z.F, and D.C. The project was supervised by K.L., Z.F., V.A.R, K.W., and C.C.H. All authors discussed the results and commented on the manuscript.

Data availability

The data that support the findings of this study are available from the corresponding author upon request.

Disclosures

The authors have declared that no conflict of interest exists

controlling infections, defective monocyte function may contribute to CF progression. In this study, we demonstrate that monocytes from CFTR$^{\Delta F508}$ mice (CF mice) show defective adhesion under flow. Transplanting CF mice with wild-type (WT) bone marrow after sublethal irradiation replaced most (60–80%) CF monocytes with WT monocytes, significantly improved survival, and reduced inflammation. WT/CF mixed bone marrow chimeras directly demonstrated defective CF monocyte recruitment to the bronchoalveolar lavage and the intestinal lamina propria in vivo. WT mice reconstituted with CF bone marrow also show lethality, suggesting that the CF defect in monocytes is not only necessary but also sufficient to cause disease. We also showed that monocyte-specific knockout of CFTR retards weight gains and exacerbates DSS-induced colitis. Our findings show that providing WT monocytes by bone marrow transfer rescues mortality in CF mice, suggesting that similar approaches may mitigate disease in CF patients.

Introduction

Cystic fibrosis (CF) is one of the most common monogenic diseases (more than 70,000 cases worldwide, ~1,000 new cases each year) (1), which is caused by variations in the cystic fibrosis transmembrane conductance regulator (CFTR) gene. CFTR is an anion-conducting transmembrane channel that is very important in mucus formation and the ion homeostasis of cells (2). More than 2000 gene variants have been identified, which are grouped into six types of mutations (2). In humans, CF disease is dominated by lung and pancreas pathologies. The dominant pathology in the lung is inflammation caused by failure to clear microorganisms and the generation of a toxic pro-inflammatory microenvironment (2–4). CFTR dysfunction in the pancreas results in pancreatic insufficiency in most CF patients (2).

CFTR mutations result in mucus dysfunction (5) and impaired mucociliary clearance in sino-pulmonary tissue. The resulting viscous mucus becomes infected with pathogens, such as *Pseudomonas aeruginosa* (6–9), *Staphylococcus aureus* (10, 11), *Haemophilus influenza* (12), and *Aspergillus* species (13). These recurrent infections greatly exacerbate the symptoms of CF (4, 5, 14) and impact the patients' quality of life. Current clinical management of CF includes prophylactic (flucloxacillin) and therapeutic antibiotics (nebulized tobramycin, colistin, and aztreonam), DNAse (Dornase alfa), CFTR potentiators and correctors (Ivacaftor, Lumacaftor), and mucus thinners (Hypertonic saline) (15). Although progress has been made (16), there is currently no cure for CF.

There are several animal models of CF, some of which mimic human pathology. In several mouse models of CF (17, 18), homologues of common human CFTR mutations have been knocked into the mouse CFTR locus. For the present mechanistic study, we use the CFTR$^{\Delta F508}$ mouse (19), a widely used and well-accepted mouse model of CF (20, 21), although it is dominated by intestinal pathology, mucus accumulation in the crypts of Lieberkühn, goblet cell hypertrophy, hyperplasia, and eosinophilic concretion in the crypts, ultimately resulting in constipation, rectal prolapse, ileus and death (22).

A recent study reported that mutations of CFTR commonly found in CF patients cause a profound monocyte adhesion defect (23, 24). The authors demonstrated expression of CFTR in human monocytes and found a significant defect of their integrin activation and static

adhesion. A similar defect of static adhesion was reported in CFTR$^{\Delta F508}$ mouse monocytes, resulting in a ~60% (human) or ~40% (mouse) loss of monocyte static adhesion. Adhesion under flow was not studied. Activation of the three main monocyte integrins (25), β_2 ($\alpha_L\beta_2$, $\alpha_M\beta_2$) and α_4 ($\alpha_4\beta_1$), was found to be defective. Remarkably, this defect is restricted to monocytes, with no defect in neutrophils and a minor defect (~20–30%) in lymphocytes. These features and the molecular mechanism make it different from the known leukocyte adhesion deficiencies (LAD) I, II, and III (26), suggesting that CF is associated with a new leukocyte adhesion deficiency, LAD IV (24).

Monocytes are important guardians of epithelial surfaces. They serve by directly secreting cytokines (27) and killing pathogens (28, 29). Monocytes can differentiate into macrophages and inflammatory dendritic cells (30). Macrophages clear apoptotic debris (efferocytosis), secrete cytokines for tissue homeostasis and survey the environment (31). When macrophages detect pathogens or danger signals, they directly phagocytose and kill bacteria (29, 32). They also produce many inflammatory cytokines and chemokines that orchestrate the recruitment of other immune and inflammatory cells (27), which are involved in the inflammatory antimicrobial response, wound healing, and fibrosis (33). Monocyte-derived dendritic cells migrate to the draining lymph nodes, where they present antigens to CD4 and CD8 T cells and thus control the adaptive immune response.

Given the expression of CFTR in monocytes (23), and given the monocyte adhesion defect, we reasoned that monocyte recruitment to mucosal sites might be defective in CFTR$^{\Delta F508}$ mice (CF mice), resulting in weakened host defense and increased pathogen burden. Here, we report that the monocyte recruitment is indeed defective. We reasoned that correcting CFTR in monocytes might improve CF disease burden and clinical outcomes. To test this, we performed bone marrow transplantation (BMT) to generate mice that were defective in CFTR in hematopoietic cells, non-hematopoietic cells, both, or neither. We observed improvement of CF symptoms and longer survival in mice that received wild-type (WT) bone marrow (BM). Mechanistically, we show that CF monocytes have a severe recruitment defect to the intestinal lamina propria and the bronchoalveolar space. Since it is now possible to correct genetic defects in hematopoietic stem cells (HSCs) (34, 35), these data suggest that autologous transfer of engineered HSCs or allogeneic BMT should be attempted in patients with CF.

Materials and Methods

Reagents

Recombinant mouse P-selectin-Fc, ICAM-1-Fc, and CCL2 were purchased from R&D Systems. Casein blocking buffer, Penicillin-Streptomycin solution, pHrodo™ Red *Staphylococcus aureus* bioparticles, and dextran sulfate sodium (DSS) were purchased from Thermo Fisher Scientific. Roswell Park Memorial Institute (RPMI) medium 1640 without phenol red, phosphate-buffered saline (PBS) without Ca^{2+} and Mg^{2+}, Hanks' balanced salt solution (HBSS) with phenol red without Ca^{2+} and Mg^{2+} were purchased from Gibco. Fetal bovine serum (FBS) and human serum albumin (HSA) were purchased from Gemini Bio Products. Phorbol 12-myristate 13-acetate (PMA), Type VIII collagenase, Dnase, and N-Acetyl-L-cysteine I were purchased from Sigma-Aldrich. Phycoerythrin (PE) or PE-Cyanine

7 (Cy7)-conjugated anti-CD115 antibody (clone AFS98), Alexa Fluor 647 (AF647), AF700, or Brilliant Violet 650 (BV650)-conjugated anti-Ly6G antibody (clone 1A8), BV785-conjugated anti-CD11b antibody (clone M1/70), BV605-conjugated anti-CD11c antibody (clone N418), BV570-conjugated anti-Ly6C antibody (clone HK1.4), BV711-conjugated anti-TCRβ antibody (clone H57–597), Allophycocyanin (APC)-conjugated anti-CD117 antibody (clone 2B8), APC-Cy7-conjugated anti-CD19 antibody (clone 6D5), PE-conjugated anti-Ly6A/E antibody (clone D7), BV650-conjugated anti-NK1.1 antibody (clone PK136), PE-conjugated anti-F4/80 antibody (clone BM8), FITC-conjugated anti-CCR2 antibody (clone SA203G11), unconjugated anti-CD11b blocking antibody (clone M1/70), and unconjugated CD18 blocking antibody (clone M18/2) were purchased from Biolegend. Ghost Dye™ Violet 510 was purchased from Tonbo biosciences. Fluorescein (FITC)-conjugated anti-CD45.1 antibody (clone A20) was purchased from BD Biosciences. Peridinin Chlorophyll Protein Complex (PerCP)-Cy5.5-conjugated anti-CD45.2 antibody (clone 104), PE-eFluor610-conjugated anti-CD4 antibody (clone GK1.5), eFluor450-conjugated anti-CD8a antibody (clone 53–6.7) were purchased from eBioscience. Red blood cell (RBC) lysis buffer was purchased from Invitrogen. iC3b was purchased from Complement Technology. EasySep™ Mouse Monocyte Isolation Kit was purchased from STEMCELL Technologies.

Mice

C57BL/6J WT mice (000664; JAX), DsRed mice (006051; JAX; WT C57BL/6J background), CD45.1 mice (002014; JAX; WT C57BL/6J background), $CFTR^{\Delta F508}$ or CF mice (002515; JAX; C57BL/6J background), and CSFR1-cre mice (029206; JAX; C57BL/6J background) were obtained from the Jackson Laboratory. $CFTR^{flox/flox}$ ($Cftr^{tm1Cwr}$; C57BL/6J background) mice were developed by and obtained from the Cystic Fibrosis Mouse Models Core at Case Western Reserve University. CD45.1/CD45.2 mice were bred by C57BL/6J WT and CD45.1 mice. Mice were fed a standard rodent chow diet and were housed in microisolator cages in a pathogen-free facility in the La Jolla Institute for Immunology or UConn Health. Mice were euthanized by CO_2 inhalation. All experiments followed guidelines of the La Jolla Institute for Immunology and UConn Health Animal Care and Use Committee, and approval for the use of rodents was obtained from the La Jolla Institute for Immunology and UConn Health according to criteria outlined in the Guide for the Care and Use of Laboratory Animals from the National Institutes of Health.

BMT

WT or CF Recipients (C57BL/6J background littermates, male or female, one-month-old) were irradiated in two doses of 550 or 350 rads each (for a total of 1,100 or 700rads) four hours apart (RS-2000 X-Ray irradiator, Rad Source). Bone marrow cells from both femurs and tibias of donor mice (WT or CF mice, sex-matched, one-month-old) were collected under sterile conditions. Bones were centrifuged for the collection of marrow, and unfractionated bone marrow cells were washed, resuspended in PBS, injected retro-orbitally into the lethally irradiated mice (one donor to five recipients). Recipient mice were housed in a barrier facility under pathogen-free conditions before and after bone marrow transplantation. After bone marrow transplantation, mice were provided autoclaved acidified water with antibiotics (trimethoprim-sulfamethoxazole) and were fed autoclaved food. The

survival of mice was monitored. Mice were used for further experiments eight weeks after bone marrow reconstitution. In some experiments, DsRed WT mice were used as recipients or donors to test the reconstructive rate of BMT by flow cytometry.

In the mixed chimeric BMT, CD45.1/CD45.2 or WT C57BL/6J mice (eight weeks old males) were irradiated in two doses of 550 rads each (for a total of 1,100 rads) four hours apart (RS-2000 X-Ray irradiator, Rad Source). Bone marrow cells from both femurs and tibias of donor mice (CF male and CD45.1 WT male, eleven weeks old) were collected under sterile conditions. Bones were centrifuged for the collection of marrow, and unfractionated bone marrow cells were washed, resuspended in PBS, mixed at a ratio of 1:1 or 1:2, confirmed by flow cytometry, and injected retro-orbitally into the lethally irradiated mice (one donor to five recipients). Recipient mice were housed in a barrier facility under pathogen-free conditions before and after bone marrow transplantation. After bone marrow transplantation, mice were provided autoclaved acidified water with antibiotics (trimethoprim-sulfamethoxazole) and were fed autoclaved food. Mice were used for further experiments eight weeks after bone marrow reconstitution.

Bodyweight and hematology

The bodyweight of aged CF and WT littermates (40–72 weeks) and young $CFTR^{flox/flox}$ Csfr1-$cre^{+/-}$ and $CFTR^{flox/flox}$ Csfr1-$cre^{-/-}$ littermates (age from 3–6 weeks) were recorded. Blood counts of WT or CF littermates (age from 10–25 weeks) were taken via retro-orbital bleeding and analyzed by an automatic analyzer (Hemavet 950FS, DREW Scientific). Mice were anesthetized by the inhalation of the isoflurane/oxygen gas mixture during the bleeding.

Flow cytometry

Blood was obtained by cardiac puncture with an ethylenediaminetetraacetic acid (EDTA)-coated syringe. Red blood cells were lysed in RBC Lysis Buffer according to the manufacturer's protocol. Lungs were lavaged with PBS containing 2mM EDTA, dissociated by gentleMACS™ Dissociator (Miltenyi), and filtered through a 70 μm strainer. Ten centimeters of small intestines from the end of the stomach, which contains the duodenum and a part of the jejunum, were collected. For the preparation of lamina propria (LP) cells, fat and connective tissue were removed from the intestines. Intestines were opened longitudinally, cut into 1-cm pieces, and washed 3× 10 minutes in HBSS containing 5% FBS, 2 mM EDTA, 100 mM N-acetyl cysteine, and 10 mM HEPES to remove mucus and epithelial cells. Tissue was digested with 1 mg/mL collagenase VIII (Sigma) and 20 μg/mL DNase I (Sigma) for 20 minutes at 37°C. Digested material was dissociated by gentleMACS™ Dissociator (Miltenyi) and filtered through a 70 μm strainer. Bone marrow cells were collected from both femurs and tibias. In some experiments, mice were challenged intranasally with mouse CCL2 100ng/mouse 12 hours prior to the harvest. Blood was collected via retro-orbital bleeding. Bronchoalveolar lavage fluid (BAL) was collected by intratracheal lavage with PBS before the collection of lungs.

All samples were collected in PBS with 2 mM EDTA to prevent cation-dependent cell-cell adhesion and were stored on ice during transportation, staining, and analysis.

Cells were resuspended in 100 μl flow staining buffer (1% BSA and 0.1% sodium azide in PBS). Cells were stained with Ghost Dye™ Violet 510 for analysis of viability. Fcγ receptors were blocked for 15 min, and surface antigens on cells were stained for 30 min at 4°C with directly conjugated fluorescent antibodies (anti-CD45.1-FITC, anti-CD45.2-PerCP-Cy5.5, anti-CD11b-BV785, anti-CD11c-BV605, anti-CD115-PE-Cy7, anti-Ly6C-BV570, anti-Ly6G-AF700, anti-TCRβ-BV711, anti-CD4-PE-eFluor610, anti-CD8a-eFluor450, anti-CD19-APC-Cy7, anti-CD117-APC, anti-Ly6A/E-PE, and anti-NK1.1-BV650 for blood and bone marrow cells; anti-CD45.1-FITC, anti-CD45.2-PerCP-Cy5.5, anti-CD11b-BV785, anti-CD11c-BV605, anti-CD115-PE-Cy7, anti-Ly6C-BV570, anti-Ly6G-AF700, anti-TCRβ-BV711, anti-CD4-PE-eFluor610, anti-CD8a-eFluor450, anti-CD19-APC-Cy7, anti-F4/80-PE, and anti-NK1.1-BV650 for BAL, lung, and LP cells). Forward and side-scatter parameters were used for the exclusion of doublets from the analysis. Cell fluorescence was assessed with an LSRII (BD Biosciences) and was analyzed with FlowJo (BD, version 10.4). Lung and LP monocytes or macrophages were normalized by blood monocytes to eliminate the reconstructive rate difference of WT and CF BM after BMT.

In CCR2 expression experiment, blood was obtained by retro-orbital bleeding. Red blood cells were lysed in RBC Lysis Buffer according to the manufacturer's protocol. Fcγ receptors were blocked for 15 min, and surface antigens on cells were stained for 30 min at 4°C with directly conjugated fluorescent antibodies (anti-Ly6G-BV650, anti-CD115-PE, and anti-CCR2-FITC). Forward and side-scatter parameters were used for exclusion of doublets from the analysis. Cell fluorescence was assessed with an LSRII (BD Biosciences) and was analyzed with FlowJo (BD, version 10.4). Monocytes were gated as $CD115^{+}Ly6G^{-}$ cells, and the median fluorescence intensities (MFI) of FITC were used to quantify CCR2 expression.

In the phagocytosis assay, pHrodo™ Red *Staphylococcus aureus* bioparticles (1.33 mg/mL) were immobilized by iC3b (0.33 mg/mL) at 4ºC overnight and washed twice with PBS before use. Bone marrow cells were collected from both femurs and tibias of WT and CF mice. Monocytes were purified using EasySep™ Mouse Monocyte Isolation Kit according to the manufacturer's protocol. Purified monocytes were resuspended in 1.5×10^{6}/mL, incubated with 10 μM PMA and 20 μg/mL CD11b, CD18 blocking antibodies, or isotype controls at room temperature (RT), 300 rpm (plate shaker) for 15 minutes, and incubated with iC3b-immobilized pHrodo™ Red *Staphylococcus aureus* bioparticles (66.6 μg/mL) at 37 ºC, 100 rpm (shaking incubator) for one hour. After two washes with 1% PFA and one wash with PBS with 2 mM EDTA, cell fluorescence was assessed with an LSRII (BD Biosciences) and was analyzed with FlowJo (BD, version 10.4). The MFI of pHrodo™ Red *Staphylococcus aureus* bioparticles in monocytes was used to quantify phagocytosis. The MFI was normalized to the CD18 blockade sample of each mouse to eliminate the background of β2 integrin-independent phagocytosis.

Histology

Intestines were rinsed, opened on the anti-mesenteric side, cut into three strips, and placed in parallel on a biopsy pad in a cassette. Samples were then fixed in zinc formalin, embedded

in paraffin, and cut into 3- to 5-μm sections. The tissues were stained with hematoxylin and eosin (H&E) and periodic acid-Schiff (PAS) for histological assessment by a single investigator who was blinded to the experimental design. Slides were digitized on AxioScan Z1 slide scanner using 40× 0.95NA objective (Zeiss). The height of intestinal villi and crypt and the percentage of intestinal crypts that contain mucus were quantified in ZEN Blue software (Zeiss).

Microfluidic perfusion assay

The assembly of the microfluidic devices used in this study and the coating of coverslips with recombinant mouse P-selectin-Fc and ICAM-1-Fc have been described previously (36–39). Briefly, cleaned coverslips were coated with P-selectin-Fc (2 μg ml^{-1}) and ICAM-1-Fc (10 μg ml^{-1}) for 2 hours and then blocked for 1 hour with casein (1%) at RT. After coating, coverslips were sealed to polydimethylsiloxane chips by magnetic clamps to create flow chamber channels ~29 μm high and ~300 μm across. By modulating the pressure between the inlet well and the outlet reservoir, 6 dyn cm^{-2} wall shear stress was applied in all experiments.

For the in vitro adhesion assay of monocytes, isolated mouse BM cells (10^7 cells ml^{-1}) from WT or CF mice were incubated with PE-conjugated anti-CD115 antibody and AF647-conjugated anti-Ly6G antibody for 10 minutes at RT and perfused through the microfluidic device over a substrate of recombinant mouse P-selectin-Fc and recombinant mouse ICAM-1-Fc at a wall shear stress of 6 dyn cm^{-2}. After cells were rolling on the substrate, 100 ng ml^{-1} mouse CCL2 was perfused. The processes of rolling and arrest were recorded by epifluorescence microscopy using an Olympus IX71 inverted microscope equipped with a 40×0.95NA objective.

DSS-induced colitis

Colitis was induced by adding 2% DSS in the drinking water for five days, followed by regular water. Mice (males, 11 weeks old) were monitored and weighed every day for two weeks and then sacrificed. Bodyweight data is normalized by the initial body weight to determine the weight lost.

Statistics

Statistical analysis was performed with Prism 6 (GraphPad). Data are presented as survival curve (Fig. 1A,2A,3A), mean ± SD plus individual data points (Fig. 1B–F, I–L,2C,D,F,3C–E,4B–G,5, Supplemental Figure 3,2B,C,E), and individual data points with linear regressions (Supplemental Figure 1). Survival curves were compared using the Gehan-Breslow-Wilcoxon test. The means for the data sets were compared using the Student t-tests with equal variances. Linear regressions were compared using the F-test. P values less than 0.05 were considered significant.

Results

As expected, CF mice died spontaneously under specific-pathogen-free conditions. The first mice succumbed at 23 days of age, with half of all deaths occurring by 40 days and ~91%

CF mice succumbing by 59 days (Fig. 1A). Like WT ($CFTR^{WT/WT}$) mice, heterozygous mice ($CFTR^{\Delta F508/WT}$) survived for at least 110 days. At the same age (paired comparison of littermates), CF mice had significantly lower body weights (Fig. 1B, Supplemental Figure 1) and significantly elevated blood leukocyte counts (Fig. 1C). Monocytes, lymphocytes, and neutrophils were all elevated (Fig. 1D–F).

Adhesion defect under flow and phagocytosis defect of CF monocytes

Previous studies (23) showed that CF monocytes have an adhesion defect under static conditions. However, in vivo, monocytes must adhere to endothelial cells under flow conditions. To test monocyte adhesion under flow, we used a microfluidic device (36, 40). The best monocyte-specific marker is CD115 (Colony-stimulating factor 1 receptor, CSF1R), and the best marker for neutrophils is Ly6G (Fig. 1G). Using monoclonal antibodies to CD115 (red) and Ly6G (cyan), we visualized monocytes and neutrophils in flow chambers coated with P-selectin (to support rolling (36, 41, 42)) and ICAM-1 (to bind β2 integrins and support arrest (36, 42)) (Fig. 1H). In these experiments, arrest was triggered by infusing CCL2 (Chemokine C-C motif ligand 2, also knowns as monocyte chemoattractant protein-1, MCP-1) at a concentration of 100 $ng{\cdot}mL^{-1}$. This is known to trigger rapid integrin activation and arrest of monocytes (43, 44). The same number of WT or CF BM cells (5×10^7 mL^{-1}) were perfused in the flow chambers. Rolling and arrest were monitored by epifluorescence microscopy (Supplemental Movie 1). The total number of cells (monocytes plus neutrophils) per field-of-view was the same in flow chambers perfused with WT or CF BM cells. The number of arrested WT, but not CF monocytes, doubled in response to CCL2 (Fig. 1I, J). We also assessed expression of CCR2, the CCL2 receptor, on blood monocytes from WT and CF mice and found no significant difference (Fig. 1K). Thus, we conclude that CCL2-induced arrest under flow is completely abolished in CF monocytes.

Besides adhesion, complement-mediated phagocytosis of monocyte also depends on β2 integrin activation (45). Complement-mediated phagocytosis of C3b-coated beads and *Pseudomonas aeruginosa* has been reported to be deficient in blood monocytes from CF patients (46). We tested whether purified monocytes from CF mice have a similar defect in phagocytizing *Staphylococcus aureus* bioparticles (Fig. 1L). We found that PMA pre-stimulated monocytes from CF mice phagocytized significantly fewer iC3b-immobilized *Staphylococcus aureus* bioparticles compared to monocytes from WT mice on a per-cell basis. This phagocytosis defect in CF monocytes is Mac-1 (integrin $\alpha_M\beta_2$, CD11b/CD18) dependent because CD11b or CD18 antibody blockade reduced the phagocytosis of WT monocytes, but not the phagocytosis of CF monocytes.

Transplanting WT BM relieves CF disease in mice

Histological assessment of the small intestine revealed the previously described increased crypt depth and villus height in CF mice (Supplemental Figure 2A). For both parameters, the differences between CF and WT mice were significant (Supplemental Figure 2B, C). CF mice also showed more mucus accumulation in the crypts of Lieberkühn than WT mice (Supplemental Figure 2D), resulting in a significantly larger percentage of crypts containing mucus (Supplemental Figure 2E).

Next, we asked whether reconstituting CFTR in hematopoietic stem cells (and therefore monocytes) was sufficient to improve the health of CF mice. To this end, we conducted BMT by injecting sterile WT or CF (control) BM cells into sub-lethally (700 rads) irradiated CF recipient mice. Reconstituting CF mice with WT BM resulted in 60–80% WT monocytes (Supplemental Table 1) and significantly prolonged their survival (Fig. 2A). The median survival time increased from 34 to 99 days, and 33% of the mice survived for up to 225 days. Interestingly, all mice that survived to 110 days (80 days after BMT) remained alive for the entire experiment. Pathologic evaluation of the bone marrow-transplanted mice showed that reconstituting CF mice with WT BM restored the crypt height defect (Fig. 2B, C), but not the villus height defect (Fig. 2D). This treatment also reduced the mucus percentage as assessed by histology (Fig. 2E, F).

Transplanting CF BM induces disease in WT mice

In a reverse approach, we tested whether the CFTR-dependent monocyte adhesion defect was sufficient to confer disease to WT mice. We reconstituted lethally (1100 rads) irradiated WT mice with CF or WT (control) BM (Fig. 3A). This is a model of complete bone marrow replacement, and almost all hematopoietic cells are donor-derived. The reconstitution efficiency of BM in mice upon the 1100 rads lethally irradiation was >90% (Supplemental Table 1). The epithelial cells are host-derived and thus retain intact, functional CFTR. All WT to WT bone marrow transplanted control mice survived for the entire duration of the experiment (232 days), but half of the mice that were reconstituted with CF BM succumbed by 41 days.

Reconstituting WT mice with CF BM induced the crypt height defect (Fig. 3B, C), but did not change villus height or mucus percentage (Fig. 3D, E). Thus, we conclude that $CFTR^{\Delta F508}$ in hematopoietic cells (by BMT of $CFTR^{\Delta F508}$ cells) might induce CF disease in WT mice. Taken together, these data show that the CFTR defect in bone marrow cells may be both necessary and sufficient to drive CF disease in mice. CFTR-dependent monocyte adhesion defect may contribute to CF pathology. Moreover, we observed an increased number of CCR2+ $Ly6C^{hi}$ inflammatory monocytes in the bone marrow of CF mice compared to controls (Supplemental Figure 3). This pro-inflammatory phenotype of monocytes in CF mice may also contribute to CF pathology.

Recruitment defect of CF monocytes in vivo

Having shown the monocyte arrest defect under flow, we next asked whether this arrest defect translated into an in vivo monocyte recruitment defect of CF monocytes. To stringently investigate the recruitment of monocytes to the intestine and lung, we used mixed BM chimeras (36). In these experiments, lethally irradiated WT mice were reconstituted with both WT and CF BM (Fig. 4A) at an approximately 1:1 ratio. WT cells were CD45.1 and CF cells were CD45.2, two functionally equivalent alleles of CD45 that are distinguishable by flow cytometry. Both monocytes and macrophages were identified by flow cytometry. In unchallenged mice, there was no difference in the number of WT and CF monocytes in the lung (Fig. 4B), but the lungs contained significantly more WT than CF macrophages (Fig. 4C). This finding suggests that the monocyte-to-macrophage differentiation, a process known to require integrin signaling (47, 48), may be defective

in CF monocytes. To directly test monocyte recruitment in vivo, we challenged mixed CF/WT bone marrow chimeric mice with intranasal CCL2. Significantly more WT than CF monocytes appeared in the BAL, demonstrating defective CF monocyte recruitment in vivo (Fig. 4D). This was true for all monocytes and specifically the Ly6C-hi subset (Fig. 4E). In the small intestinal lamina propria, the findings were similar: we found no difference between WT and CF monocytes in unchallenged mice (Fig. 4F), but more WT than CF macrophages in lamina propria leukocytes (LPL, Fig. 4G). Taken together, these findings indicate that the CF monocyte defect manifests in defective elicited monocyte recruitment and defective monocyte to macrophage differentiation.

Monocyte specific CFTR defect leads to severe gut inflammation

To investigate the monocyte-specific contribution in CF gut inflammation, we investigated $CFTR^{flox/flox}$ Csfr1-$cre^{+/-}$ mice. Of 27 $CFTR^{flox/flox}$ Csfr1-$cre^{+/-}$ mice, three died on days 21, 26, 30, respectively. Of 29 $CFTR^{flox/flox}$ Csfr1-$cre^{-/-}$ littermates, one died on day 31. We observed a slight but significant decrease in body weight gain of $CFTR^{flox/flox}$ Csfr1-$cre^{+/-}$ mice compared to $CFTR^{flox/flox}$ Csfr1-$cre^{-/-}$ littermates (Fig. 5A).

Next, we tested the contribution of monocyte-specific CFTR defect in a DSS-induced colitis model. We found that $CFTR^{flox/flox}$ Csfr1-$cre^{+/-}$ mice lose significantly more bodyweight after DSS administration compared to $CFTR^{flox/flox}$ Csfr1-$cre^{-/-}$ littermates (Fig. 5B). These results suggested that CFTR deficiency in monocytes contributes to the pathogenesis of gut inflammation.

Discussion

This study demonstrates that BMT rescues the CF phenotype in the $CFTR^{\Delta F508}$ mouse model. Although this model does not exactly recapitulate human CF disease, this fundamental discovery suggests that BMT mitigated some aspects of CF disease by restoring monocyte/macrophage function and mucosal host defense. Survival and inflammation of CF mice were both improved by the hematological reconstitution using WT BM. We show that CF monocytes fail to adhere under flow, show reduced recruitment in response to CCL2, and contribute less to macrophages in the lung and intestinal lamina propria than WT monocytes. We show that the $CFTR^{\Delta F508}$ in monocytes might be both necessary (BMT with WT bone marrow into CF mice improves the disease) and sufficient (BMT with CF bone marrow into WT mice induces the disease) for full manifestation of CF disease.

Besides the monocyte recruitment defect, CF monocytes may have other functional defects when challenged by inflammation and infections. Upon LPS stimulation, monocytes from CF patients have been reported to show reduced inflammatory cytokine expression (lower TNFα, lower IL-6, lower IL-12, lower IL-23) and increased production of anti-inflammatory IL-10 compared to WT controls (49). Taken together with our findings, this suggests complex defects encompassing monocyte arrest, recruitment, cytokine production, and differentiation into macrophages. The common denominator of these defects may be defective β_2 integrin activation in CF monocytes because β_2 integrins are known to be involved in many myeloid cell functions (50). Exactly why CF monocytes have a defect

in differentiating to macrophages is beyond the scope of the present work and will be addressed in future studies.

Whether or not CF monocytes show defective phagocytosis remains controversial. Complement-mediated phagocytosis of C3b-coated beads and *Pseudomonas aeruginosa* has been reported to be deficient in blood monocytes from CF patients (46). In another study, the phagocytosis of *Escherichia coli* was increased in CF monocytes (49). These findings suggest that some but not all phagocytosis mechanisms are affected by dysfunctional CFTR. Antigen presentation to CD4 T cells by MHC-II is decreased in CF monocytes (49). A recent study showed that WT CFTR associates with PTEN, triggering the anti-inflammatory PI3K/Akt pathway in response to Toll-like receptor 4 (TLR4). This helps enhance *Pseudomonas aeruginosa* clearance (7), suggesting a mechanism that may fail in CF patients.

CFTR is expressed in the monocyte but not the neutrophil plasma membrane (46). Consequently, CFTR deficiency did not affect the adhesion of human neutrophils (23), which are the most abundant leukocytes in human blood and play essential roles in immune defense (36). However, CFTR mRNA is expressed in human neutrophils (51). CFTR protein is found expressed in the phagolysosome membrane of neutrophils, which affects bacterial killing, degranulation, and disease outcome (51–56). Thus, correcting CFTR by BMT may also restore the function of neutrophils and improve CF by promoting bacterial killing.

Our study is not the first CF study to use BMT, but it is the first to focus on monocyte defects. Previous investigators hypothesized that stem cells may exist among lung epithelial cells (57–59) or gut epithelial cells (59, 60). These studies provided evidence that hematopoietic stem cells and multipotent mesenchymal stromal cells can home to the lung or intestine. Whether they can differentiate into functional epithelial cells is less clear. A mild but significant rescue (~10%) of epithelial electrophysiology was shown in distal colons of CF mice, which have a decrease of forskolin-induced transepithelial current compared to WT controls (59, 60). However, the epithelial reconstitution was incomplete, even under optimized conditions (57). Optimized WT to CF BMT improved bacterial clearance and survival after infection with *Pseudomonas aeruginosa (57)*. However, it is not clear whether the above clinical improvements may be due to an effect of BMT on putative epithelial stem cells. Although it has been shown that transferring nonhematopoietic BM cells can be differentiated to lung epithelial cells (61), there is no evidence showing that WT nonhematopoietic BM cells can rescue lung infections in CF mice. Importantly, at the time of these studies (47–50), the monocyte recruitment defect was not known. In light of the present findings, it seems more likely that the benefit observed in (57) was due to the functional rescue of myeloid cell function rather than epithelial cell function. A recent study supported our idea that, in a *Pseudomonas aeruginos* lung infection model, transferring CF BM to WT mice induced more death, and transferring WT BM to CF mice rescued the survival *(62)*. Results in *Pseudomonas aeruginosa*-infected *Cftr* KO and KI mice showed that *Cftr anti-inflammation/infection effect is* myeloid-specific *(62)*. These are consistent with our results.

Other studies have shown that CF macrophages exhibited pro-inflammatory cytokine expression, upregulated TLR4 signaling, and decreased anti-bacterial response after LPS stimulation compared to WT macrophages (63–65). In these studies, it is not clear whether the observed differences are a cause or a consequence of the ongoing CF disease process with infections. After transplantation of WT BM cells, the LPS-induced pro-inflammatory cytokine production in CF mice was reduced (63). However, monocyte recruitment was not studied. Myeloid cell recruitment to the lung is a multi-step process, where the myeloid cells first leave the blood compartment to appear in the lung interstitium and then must negotiate the epithelial layer to appear in the bronchoalveolar lavage (66). Our present findings suggest that the monocyte recruitment defect is localized to the transepithelial and not the transendothelial migration. The recruitment defect is not detected under homeostatic conditions but appears when mice are challenged with CCL2. CF patients likely are in a permanently challenged condition because of the bacterial load in the bronchoalveolar mucus.

Taken together, we show that restoration of WT monocytes by partial WT BMT is sufficient to improve health and survival in CF mice. Many CF patients are diagnosed at a young age, and BMT is more successful in children than in adults. Thus, partial BMT could be an appealing strategy for the management of CF disease (67). It appears that an antibody-based approach for BMT (without irradiation) may be safe and effective (68). Thus, this might be suitable to be tested for CF treatment. Unlike in malignant diseases, lethal irradiation is not required and partial restoration with 60–80% WT monocytes is sufficient. Moreover, it is now possible to correct gene defects in HSCs (34, 35) by gene therapy approaches. Thus, transfer of engineered autologous HSCs may become a practical treatment for patients with CF.

Supplementary Material

Refer to Web version on PubMed Central for supplementary material.

Acknowledgments

We thank Angela Denn from the Microscopy and Histology Core Facility at the La Jolla Institute for Immunology for her help in obtaining the scientific data presented in this paper. We thank Dr. Paul Quinton from the Department of Pediatrics in the School of Medicine at the University of California San Diego for his help in editing the manuscript. We thank Dr. Jesus Rivera-Nieves from the Inflammatory Bowel Disease Center in the Division of Gastroenterology at the University of California San Diego for his advice on histology.

This research was supported by funding from the National Institutes of Health, USA (NIH, HL078784 and R01HL145454), a Pilot & Feasibility Award from the Cystic Fibrosis Foundation (00841I221), a WSA postdoctoral fellowship and Career Development Award from the American Heart Association, USA (AHA, 16POST31160014 and 18CDA34110426), and a startup fund from UConn Health.

Abbreviations used in this article:

CF	cystic fibrosis
CFTR	cystic fibrosis transmembrane conductance regulator
BMT	bone marrow transplantation

WT	wild-type
LAD	leukocyte adhesion deficiencies
HSCs	hematopoietic stem cells
EDTA	ethylenediaminetetraacetic acid
LPL	lamina propria leukocytes
CCL2	Chemokine C-C motif ligand 2
MCP-1	monocyte chemoattractant protein-1
BAL	bronchoalveolar lavage fluid
DSS	dextran sulfate sodium
PMA	Phorbol 12-myristate 13-acetate

References

1. Foundation, C. F. https://www.cff.org/What-is-CF/About-Cystic-Fibrosis/.
2. Elborn JS 2016. Cystic fibrosis. The Lancet 388: 2519–2531.
3. Cohen TS, and Prince A. 2012. Cystic fibrosis: a mucosal immunodeficiency syndrome. Nature medicine 18: 509–519.
4. Cutting GR 2015. Cystic fibrosis genetics: from molecular understanding to clinical application. Nature reviews. Genetics 16: 45–56.
5. Ratjen F, Bell SC, Rowe SM, Goss CH, Quittner AL, and Bush A. 2015. Cystic fibrosis. Nature reviews. Disease primers 1: 15010.
6. Oliver A, Canton R, Campo P, Baquero F, and Blazquez J. 2000. High frequency of hypermutable Pseudomonas aeruginosa in cystic fibrosis lung infection. Science 288: 1251–1254. [PubMed: 10818002]
7. Riquelme SA, Hopkins BD, Wolfe AL, DiMango E, Kitur K, Parsons R, and Prince A. 2017. Cystic Fibrosis Transmembrane Conductance Regulator Attaches Tumor Suppressor PTEN to the Membrane and Promotes Anti Pseudomonas aeruginosa Immunity. Immunity 47: 1169–1181 e1167.
8. Wood ME, Stockwell RE, Johnson GR, Ramsay KA, Sherrard LJ, Jabbour N, Ballard E, O'Rourke P, Kidd TJ, Wainwright CE, Knibbs LD, Sly PD, Morawska L, and Bell SC 2018. Face Masks and Cough Etiquette Reduce the Cough Aerosol Concentration of Pseudomonas aeruginosa in People with Cystic Fibrosis. American journal of respiratory and critical care medicine 197: 348–355. [PubMed: 28930641]
9. Rossi E, Falcone M, Molin S, and Johansen HK 2018. High-resolution in situ transcriptomics of Pseudomonas aeruginosa unveils genotype independent patho-phenotypes in cystic fibrosis lungs. Nature communications 9: 3459.
10. Jennings MT, Dasenbrook EC, Lechtzin N, Boyle MP, and Merlo CA 2017. Risk factors for persistent methicillin-resistant Staphylococcus aureus infection in cystic fibrosis. Journal of cystic fibrosis : official journal of the European Cystic Fibrosis Society 16: 681–686. [PubMed: 28446387]
11. Caudri D, Turkovic L, Ng J, de Klerk NH, Rosenow T, Hall GL, Ranganathan SC, Sly PD, Stick SM, and Arest CF 2018. The association between Staphylococcus aureus and subsequent bronchiectasis in children with cystic fibrosis. Journal of cystic fibrosis : official journal of the European Cystic Fibrosis Society 17: 462–469. [PubMed: 29274943]
12. Starner TD, Zhang N, Kim G, Apicella MA, and McCray PB Jr. 2006. Haemophilus influenzae forms biofilms on airway epithelia: implications in cystic fibrosis. American journal of respiratory and critical care medicine 174: 213–220. [PubMed: 16675778]

13. Cowley AC, Thornton DJ, Denning DW, and Horsley A. 2017. Aspergillosis and the role of mucins in cystic fibrosis. Pediatric pulmonology 52: 548–555. [PubMed: 27870227]
14. Filkins LM, and O'Toole GA 2015. Cystic Fibrosis Lung Infections: Polymicrobial, Complex, and Hard to Treat. PLoS pathogens 11: e1005258.
15. Edmondson C, and Davies JC 2016. Current and future treatment options for cystic fibrosis lung disease: latest evidence and clinical implications. Therapeutic advances in chronic disease 7: 170–183. [PubMed: 27347364]
16. Veit G, Xu H, Dreano E, Avramescu RG, Bagdany M, Beitel LK, Roldan A, Hancock MA, Lay C, Li W, Morin K, Gao S, Mak PA, Ainscow E, Orth AP, McNamara P, Edelman A, Frenkiel S, Matouk E, Sermet-Gaudelus I, Barnes WG, and Lukacs GL 2018. Structure-guided combination therapy to potently improve the function of mutant CFTRs. Nature medicine.
17. Grubb BR, and Gabriel SE 1997. Intestinal physiology and pathology in gene-targeted mouse models of cystic fibrosis. The American journal of physiology 273: G258–266. [PubMed: 9277402]
18. Keiser NW, and Engelhardt JF 2011. New animal models of cystic fibrosis: what are they teaching us? Current opinion in pulmonary medicine 17: 478–483. [PubMed: 21857224]
19. Zeiher BG, Eichwald E, Zabner J, Smith JJ, Puga AP, McCray PB Jr., Capecchi MR, Welsh MJ, and Thomas KR 1995. A mouse model for the delta F508 allele of cystic fibrosis. The Journal of clinical investigation 96: 2051–2064. [PubMed: 7560099]
20. Fiorotto R, Amenduni M, Mariotti V, Fabris L, Spirli C, and Strazzabosco M. 2018. Src kinase inhibition reduces inflammatory and cytoskeletal changes in DeltaF508 human cholangiocytes and improves cystic fibrosis transmembrane conductance regulator correctors efficacy. Hepatology 67: 972–988. [PubMed: 28836688]
21. McNeer NA, Anandalingam K, Fields RJ, Caputo C, Kopic S, Gupta A, Quijano E, Polikoff L, Kong Y, Bahal R, Geibel JP, Glazer PM, Saltzman WM, and Egan ME 2015. Nanoparticles that deliver triplex-forming peptide nucleic acid molecules correct F508del CFTR in airway epithelium. Nature communications 6: 6952.
22. Grubb BR, and Boucher RC 1999. Pathophysiology of gene-targeted mouse models for cystic fibrosis. Physiological reviews 79: S193–214. [PubMed: 9922382]
23. Sorio C, Montresor A, Bolomini-Vittori M, Caldrer S, Rossi B, Dusi S, Angiari S, Johansson JE, Vezzalini M, Leal T, Calcaterra E, Assael BM, Melotti P, and Laudanna C. 2016. Mutations of Cystic Fibrosis Transmembrane Conductance Regulator Gene Cause a Monocyte-Selective Adhesion Deficiency. Am J Respir Crit Care Med 193: 1123–1133. [PubMed: 26694899]
24. Fan Z, and Ley K. 2016. Leukocyte Adhesion Deficiency IV. Monocyte Integrin Activation Deficiency in Cystic Fibrosis. American journal of respiratory and critical care medicine 193: 1075–1077. [PubMed: 27174474]
25. Gerhardt T, and Ley K. 2015. Monocyte trafficking across the vessel wall. Cardiovascular research 107: 321–330. [PubMed: 25990461]
26. Hanna S, and Etzioni A. 2012. Leukocyte adhesion deficiencies. Annals of the New York Academy of Sciences 1250: 50–55. [PubMed: 22276660]
27. Rossol M, Heine H, Meusch U, Quandt D, Klein C, Sweet MJ, and Hauschildt S. 2011. LPS-induced cytokine production in human monocytes and macrophages. Critical reviews in immunology 31: 379–446. [PubMed: 22142165]
28. Shi C, and Pamer EG 2011. Monocyte recruitment during infection and inflammation. Nature reviews. Immunology 11: 762–774.
29. Gresnigt MS, Cunha C, Jaeger M, Goncalves SM, Malireddi RKS, Ammerdorffer A, Lubbers R, Oosting M, Rasid O, Jouvion G, Fitting C, Jong DJ, Lacerda JF, Campos A Jr., Melchers WJG, Lagrou K, Maertens J, Kanneganti TD, Carvalho A, Ibrahim-Granet O, and van de Veerdonk FL 2018. Genetic deficiency of NOD2 confers resistance to invasive aspergillosis. Nature communications 9: 2636.
30. Jakubzick CV, Randolph GJ, and Henson PM 2017. Monocyte differentiation and antigen-presenting functions. Nature reviews. Immunology 17: 349–362.
31. Ley K, Pramod AB, Croft M, Ravichandran KS, and Ting JP 2016. How Mouse Macrophages Sense What Is Going On. Frontiers in immunology 7: 204. [PubMed: 27313577]

32. Seixas E, Escrevente C, Seabra MC, and Barral DC 2018. Rab GTPase regulation of bacteria and protozoa phagocytosis occurs through the modulation of phagocytic receptor surface expression. Scientific reports 8: 12998.
33. Murray PJ, and Wynn TA 2011. Protective and pathogenic functions of macrophage subsets. Nature reviews. Immunology 11: 723–737.
34. Morgan RA, Gray D, Lomova A, and Kohn DB 2017. Hematopoietic Stem Cell Gene Therapy: Progress and Lessons Learned. Cell stem cell 21: 574–590. [PubMed: 29100011]
35. Mettananda S, Fisher CA, Hay D, Badat M, Quek L, Clark K, Hublitz P, Downes D, Kerry J, Gosden M, Telenius J, Sloane-Stanley JA, Faustino P, Coelho A, Doondeea J, Usukhbayar B, Sopp P, Sharpe JA, Hughes JR, Vyas P, Gibbons RJ, and Higgs DR 2017. Editing an alpha-globin enhancer in primary human hematopoietic stem cells as a treatment for beta-thalassemia. Nature communications 8: 424.
36. Fan Z, McArdle S, Marki A, Mikulski Z, Gutierrez E, Engelhardt B, Deutsch U, Ginsberg M, Groisman A, and Ley K. 2016. Neutrophil recruitment limited by high-affinity bent beta2 integrin binding ligand in cis. Nature communications 7: 12658.
37. Sundd P, Gutierrez E, Pospieszalska MK, Zhang H, Groisman A, and Ley K. 2010. Quantitative dynamic footprinting microscopy reveals mechanisms of neutrophil rolling. Nat Methods 7: 821–824. [PubMed: 20871617]
38. Sundd P, Gutierrez E, Petrich BG, Ginsberg MH, Groisman A, and Ley K. 2011. Live cell imaging of paxillin in rolling neutrophils by dual-color quantitative dynamic footprinting. Microcirculation 18: 361–372. [PubMed: 21418380]
39. Sundd P, Gutierrez E, Koltsova EK, Kuwano Y, Fukuda S, Pospieszalska MK, Groisman A, and Ley K. 2012. 'Slings' enable neutrophil rolling at high shear. Nature 488: 399–403. [PubMed: 22763437]
40. Fan Z, Kiosses WB, Sun H, Orecchioni M, Ghosheh Y, Zajonc DM, Arnaout MA, Gutierrez E, Groisman A, Ginsberg MH, and Ley K. 2019. High-Affinity Bent beta2-Integrin Molecules in Arresting Neutrophils Face Each Other through Binding to ICAMs In cis. Cell Rep 26: 119–130 e115.
41. Marki A, Gutierrez E, Mikulski Z, Groisman A, and Ley K. 2016. Microfluidics-based side view flow chamber reveals tether-to-sling transition in rolling neutrophils. Sci Rep 6: 28870.
42. Fan Z, Kiosses WB, Sun H, Orecchioni M, Ghosheh Y, Zajonc DM, Arnaout MA, Gutierrez E, Groisman A, Ginsberg MH, and Ley K. 2019. High-Affinity Bent β2-Integrin Molecules in Arresting Neutrophils Face Each Other through Binding to ICAMs In cis. Cell reports 26: 119–130.e115.
43. Gerszten RE, Garcia-Zepeda EA, Lim YC, Yoshida M, Ding HA, Gimbrone MA Jr., Luster AD, Luscinskas FW, and Rosenzweig A. 1999. MCP-1 and IL-8 trigger firm adhesion of monocytes to vascular endothelium under flow conditions. Nature 398: 718–723. [PubMed: 10227295]
44. Luscinskas FW, Gerszten RE, Garcia-Zepeda EA, Lim YC, Yoshida M, Ding HA, Gimbrone MA Jr., Luster AD, and Rosenzweig A. 2000. C-C and C-X-C chemokines trigger firm adhesion of monocytes to vascular endothelium under flow conditions. Annals of the New York Academy of Sciences 902: 288–293. [PubMed: 10865849]
45. Sun H, Zhi K, Hu L, and Fan Z. 2021. The Activation and Regulation of beta2 Integrins in Phagocytes and Phagocytosis. Front Immunol 12: 633639.
46. Van de Weert-van Leeuwen PB, Van Meegen MA, Speirs JJ, Pals DJ, Rooijakkers SH, Van der Ent CK, Terheggen-Lagro SW, Arets HG, and Beekman JM 2013. Optimal complement-mediated phagocytosis of Pseudomonas aeruginosa by monocytes is cystic fibrosis transmembrane conductance regulator-dependent. American journal of respiratory cell and molecular biology 49: 463–470. [PubMed: 23617438]
47. Shi C, Miley J, Nottingham A, Morooka T, Prosdocimo DA, and Simon DI 2019. Leukocyte integrin signaling regulates FOXP1 gene expression via FOXP1-IT1 long non-coding RNA-mediated IRAK1 pathway. Biochim Biophys Acta Gene Regul Mech 1862: 493–508. [PubMed: 30831269]

48. Shi C, Zhang X, Chen Z, Sulaiman K, Feinberg MW, Ballantyne CM, Jain MK, and Simon DI 2004. Integrin engagement regulates monocyte differentiation through the forkhead transcription factor Foxp1. The Journal of clinical investigation 114: 408–418. [PubMed: 15286807]
49. del Fresno C, Garcia-Rio F, Gomez-Pina V, Soares-Schanoski A, Fernandez-Ruiz I, Jurado T, Kajiji T, Shu C, Marin E, Gutierrez del Arroyo A, Prados C, Arnalich F, Fuentes-Prior P, Biswas SK, and Lopez-Collazo E. 2009. Potent phagocytic activity with impaired antigen presentation identifying lipopolysaccharide-tolerant human monocytes: demonstration in isolated monocytes from cystic fibrosis patients. Journal of immunology 182: 6494–6507.
50. Schittenhelm L, Hilkens CM, and Morrison VL 2017. beta2 Integrins As Regulators of Dendritic Cell, Monocyte, and Macrophage Function. Frontiers in immunology 8: 1866. [PubMed: 29326724]
51. Painter RG, Valentine VG, Lanson NA Jr., Leidal K, Zhang Q, Lombard G, Thompson C, Viswanathan A, Nauseef WM, Wang G, and Wang G. 2006. CFTR Expression in human neutrophils and the phagolysosomal chlorination defect in cystic fibrosis. Biochemistry 45: 10260–10269.
52. Painter RG, Bonvillain RW, Valentine VG, Lombard GA, LaPlace SG, Nauseef WM, and Wang G. 2008. The role of chloride anion and CFTR in killing of Pseudomonas aeruginosa by normal and CF neutrophils. Journal of leukocyte biology 83: 1345–1353. [PubMed: 18353929]
53. Painter RG, Marrero L, Lombard GA, Valentine VG, Nauseef WM, and Wang G. 2010. CFTR-mediated halide transport in phagosomes of human neutrophils. Journal of leukocyte biology 87: 933–942. [PubMed: 20089668]
54. Bonfield TL, Hodges CA, Cotton CU, and Drumm ML 2012. Absence of the cystic fibrosis transmembrane regulator (Cftr) from myeloid-derived cells slows resolution of inflammation and infection. Journal of leukocyte biology 92: 1111–1122. [PubMed: 22859830]
55. Ng HP, Zhou Y, Song K, Hodges CA, Drumm ML, and Wang G. 2014. Neutrophil-mediated phagocytic host defense defect in myeloid Cftr-inactivated mice. PloS one 9: e106813.
56. Pohl K, Hayes E, Keenan J, Henry M, Meleady P, Molloy K, Jundi B, Bergin DA, McCarthy C, McElvaney OJ, White MM, Clynes M, Reeves EP, and McElvaney NG 2014. A neutrophil intrinsic impairment affecting Rab27a and degranulation in cystic fibrosis is corrected by CFTR potentiator therapy. Blood 124: 999–1009. [PubMed: 24934256]
57. Duchesneau P, Besla R, Derouet MF, Guo L, Karoubi G, Silberberg A, Wong AP, and Waddell TK 2017. Partial Restoration of CFTR Function in cftr-Null Mice following Targeted Cell Replacement Therapy. Molecular therapy : the journal of the American Society of Gene Therapy 25: 654–665. [PubMed: 28187947]
58. Loi R, Beckett T, Goncz KK, Suratt BT, and Weiss DJ 2006. Limited restoration of cystic fibrosis lung epithelium in vivo with adult bone marrow-derived cells. American journal of respiratory and critical care medicine 173: 171–179. [PubMed: 16179642]
59. Bruscia EM, Ziegler EC, Price JE, Weiner S, Egan ME, and Krause DS 2006. Engraftment of donor-derived epithelial cells in multiple organs following bone marrow transplantation into newborn mice. Stem cells 24: 2299–2308. [PubMed: 16794262]
60. Bruscia EM, Price JE, Cheng EC, Weiner S, Caputo C, Ferreira EC, Egan ME, and Krause DS 2006. Assessment of cystic fibrosis transmembrane conductance regulator (CFTR) activity in CFTR-null mice after bone marrow transplantation. Proceedings of the National Academy of Sciences of the United States of America 103: 2965–2970. [PubMed: 16481627]
61. Kassmer SH, Bruscia EM, Zhang PX, and Krause DS 2012. Nonhematopoietic cells are the primary source of bone marrow-derived lung epithelial cells. Stem Cells 30: 491–499. [PubMed: 22162244]
62. van Heeckeren AM, Sutton MT, Fletcher DR, Hodges CA, Caplan AI, and Bonfield TL 2021. Enhancing Cystic Fibrosis Immune Regulation. Front Pharmacol 12: 573065.
63. Bruscia EM, Zhang PX, Ferreira E, Caputo C, Emerson JW, Tuck D, Krause DS, and Egan ME 2009. Macrophages directly contribute to the exaggerated inflammatory response in cystic fibrosis transmembrane conductance regulator−/− mice. American journal of respiratory cell and molecular biology 40: 295–304. [PubMed: 18776130]

64. Zhang PX, Cheng J, Zou S, D'Souza AD, Koff JL, Lu J, Lee PJ, Krause DS, Egan ME, and Bruscia EM 2015. Pharmacological modulation of the AKT/microRNA-199a-5p/CAV1 pathway ameliorates cystic fibrosis lung hyper-inflammation. Nature communications 6: 6221.

65. Di Pietro C, Zhang PX, O'Rourke TK, Murray TS, Wang L, Britto CJ, Koff JL, Krause DS, Egan ME, and Bruscia EM 2017. Ezrin links CFTR to TLR4 signaling to orchestrate anti-bacterial immune response in macrophages. Scientific reports 7: 10882.

66. Reutershan J, Morris MA, Burcin TL, Smith DF, Chang D, Saprito MS, and Ley K. 2006. Critical role of endothelial CXCR2 in LPS-induced neutrophil migration into the lung. The Journal of clinical investigation 116: 695–702. [PubMed: 16485040]

67. Gupta V, Eapen M, Brazauskas R, Carreras J, Aljurf M, Gale RP, Hale GA, Ilhan O, Passweg JR, Ringden O, Sabloff M, Schrezenmeier H, Socie G, and Marsh JC 2010. Impact of age on outcomes after bone marrow transplantation for acquired aplastic anemia using HLA-matched sibling donors. Haematologica 95: 2119–2125. [PubMed: 20851870]

68. Palchaudhuri R, Saez B, Hoggatt J, Schajnovitz A, Sykes DB, Tate TA, Czechowicz A, Kfoury Y, Ruchika F, Rossi DJ, Verdine GL, Mansour MK, and Scadden DT 2016. Non-genotoxic conditioning for hematopoietic stem cell transplantation using a hematopoietic-cell-specific internalizing immunotoxin. Nature biotechnology 34: 738–745.

Key Points

1. Monocytes from CFTR$^{\Delta F508}$ mice have a defect in β2 integrin-dependent adhesion.
2. Transfering WT bone marrow rescues CF disease.
3. Monocyte-specific CFTR KO retards weight gains and exacerbates DSS-induced colitis

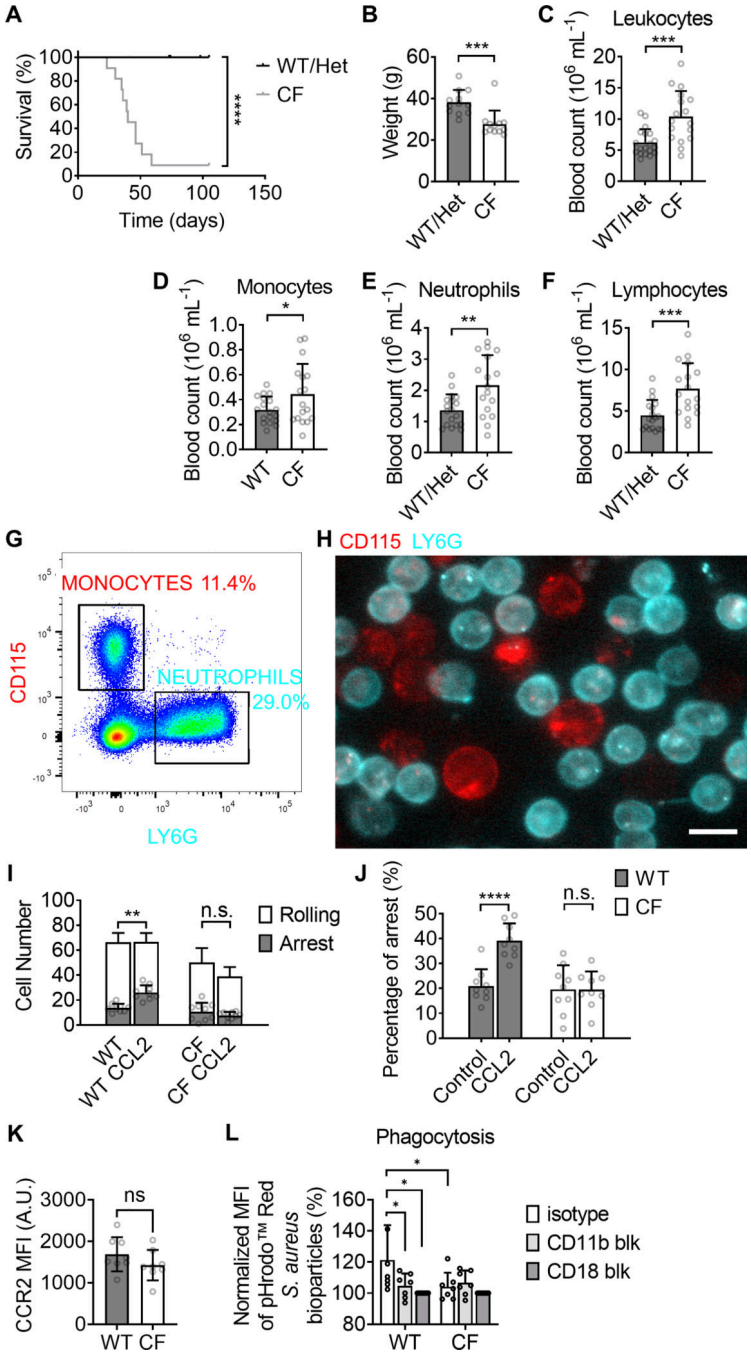

FIGURE 1.

Leukocytosis and monocyte adhesion and phagocytosis deficiency in CFTR$^{\Delta F508}$ (CF) mice. (**A-B**) the survival curve (A, n=21 WT and 11 CF) and weight (B, n=12) of CF and WT mice. (**C-F**) Hematology for total leukocytes (C), monocytes (D), neutrophils (E), and lymphocytes (F) in CF mice (n=17) compared to WT controls (n=18). (**G-H**) Monocytes and neutrophils in bone marrow (BM) cells are distinguished by staining of CD115 and Ly6G staining, respectively, in flow cytometry (G) and by fluorescence microscopy in a microfluidic flow chamber (H). Both monocytes (red) and neutrophils (cyan) adhered on the

substrate of P-selectin/ICAM-1 at a shear stress of 6 dyn·cm^{-2} (H). The scale bar is 10 μm. (**I**-**J**) Number of rolling (white) and arrested monocytes at rest and after infusion of CCL2 (100 ng·mL^{-1}) (I). The percentage of arrested as a fraction of all monocytes in a field of view (J) for WT and CF monocytes with or without the stimulation of CCL2. Mean±SD of n=9 fields-of-view. (K) CCR expression of WT and CF blood monocytes. Mean±SD of n=9 mice. (**L**) The MFI of phagocytized pHrodo™ Red *Staphylococcus aureus* bioparticles in PMA-stimulated monocytes purified from WT or CF BM in presents with isotype control (open boxes), CD11b blocking antibody (light grey boxes), or CD18 blocking antibody (dark grey boxes). Mean±SD of monocytes from n=9 mice. n.s. $p>0.05$, *$p<0.05$, **$p<0.01$, ***$p<0.001$, ****$p<0.0001$ by Gehan-Breslow-Wilcoxon test (A) and student T-test (B-F,I-L).

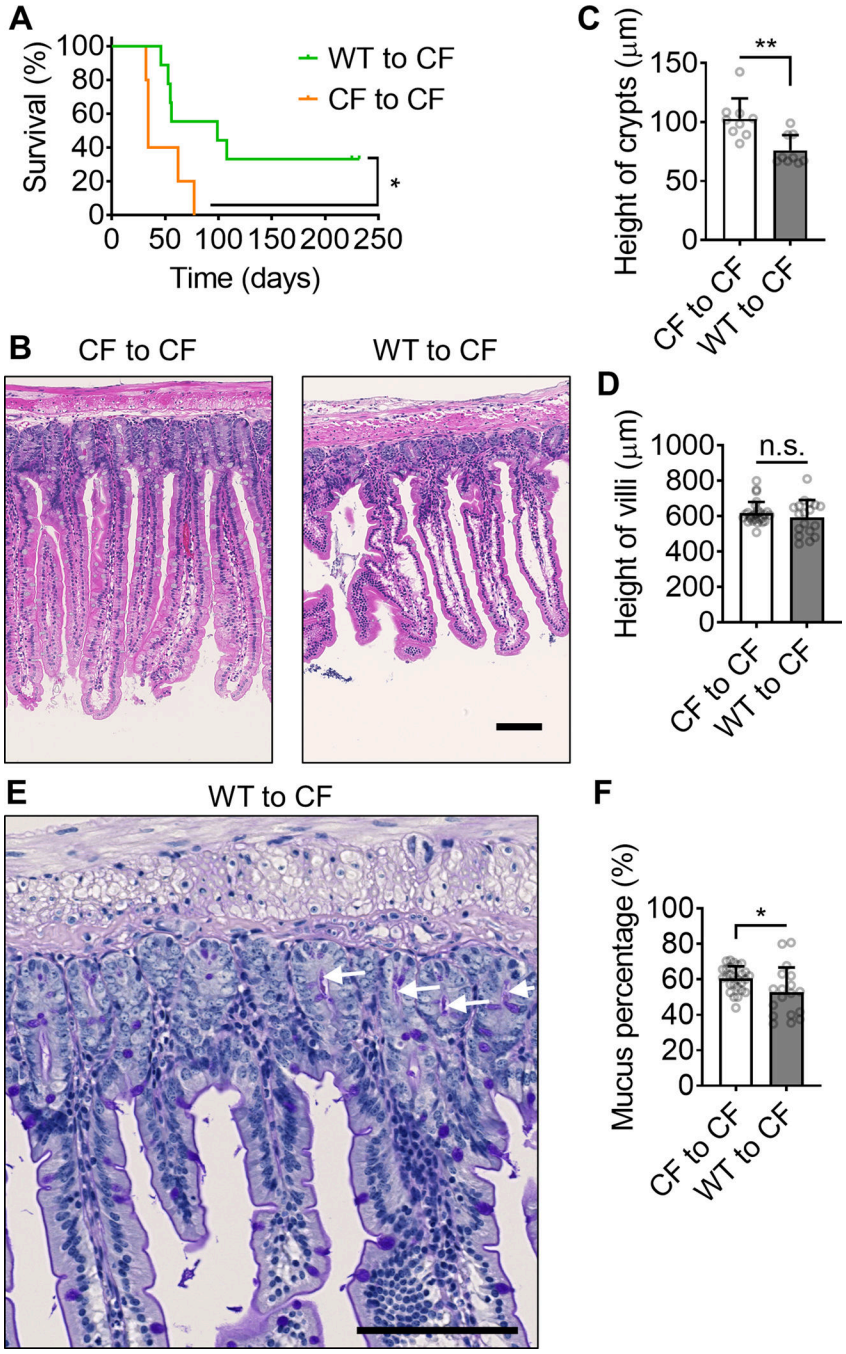

FIGURE 2.

WT Bone marrow transplantation partially rescues the survival and intestine inflammation in CFTR$^{\Delta F508}$ mice. (**A**) the survival curve of CFTR$^{\Delta F508}$ mice (700 rads) transplanted with WT (green curve, n=9;) or CFTR$^{\Delta F508}$ (orange curve, n=5) BM. (**B**) Typical H&E staining images of intestines from CFTR$^{\Delta F508}$ mice transplanted with CFTR$^{\Delta F508}$ or WT BM. (**C**-**D**) Quantification of crypts (C, Mean±SD of n=9) and villi (D, Mean±SD of n=27) height of intestines from CFTR$^{\Delta F508}$ mice transplanted with CFTR$^{\Delta F508}$ or WT BM. n=9. (**E**) A typical PAS staining image of intestine from a CFTR$^{\Delta F508}$ mouse transplanted with WT

BM. White arrows indicate mucus in crypts. (**F**) Percentage of intestine crypts that contain mucus in it. $CFTR^{\Delta F508}$ mice are transplanted with WT or $CFTR^{\Delta F508}$ BM. Mean±SD of n=27. n.s. $p>0.05$, *$p<0.05$, **$p<0.01$in the Gehan-Breslow-Wilcoxon test (A) and student t-test (C-D,F). Scale bars are 100 μm.

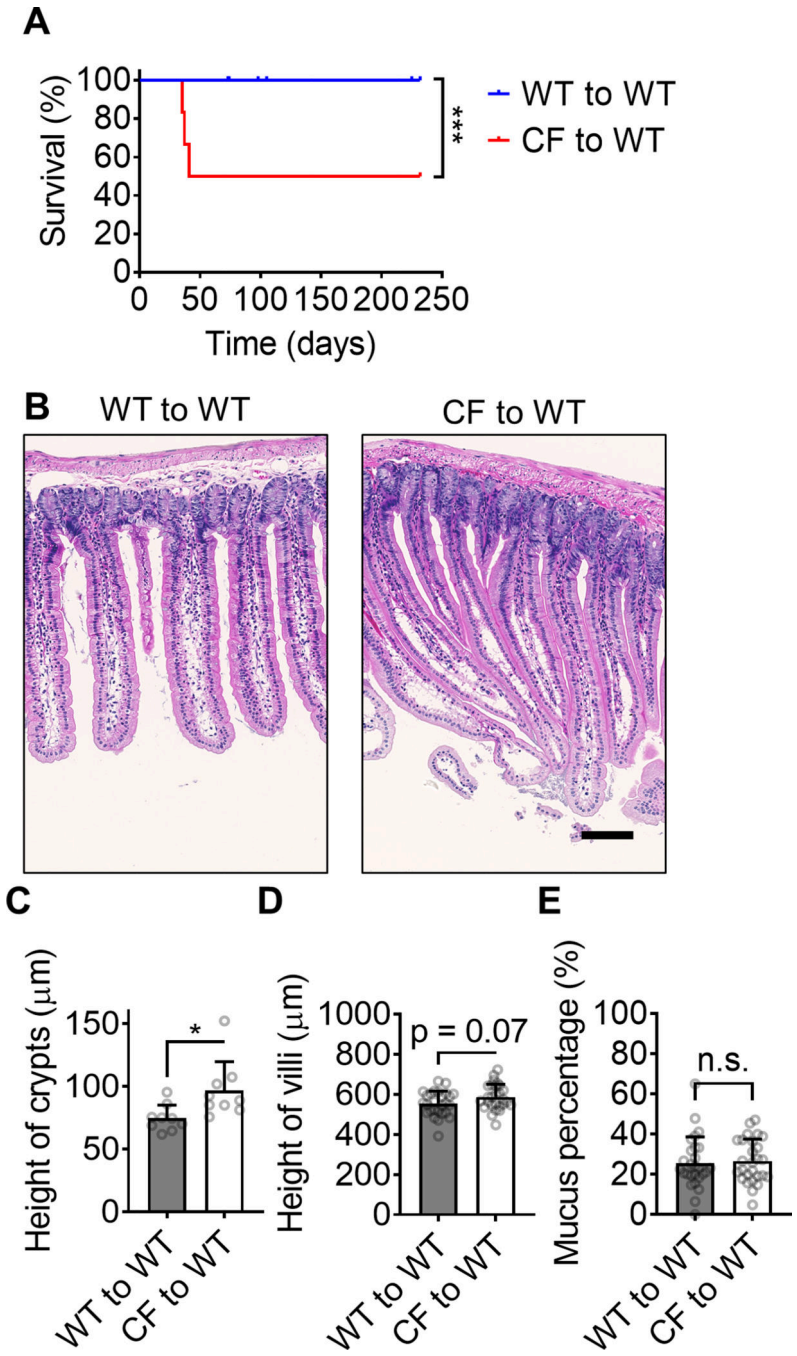

FIGURE 3.

CFTR$^{\Delta F508}$ Bone marrow transplantation induces the disease in WT mice. (**A**) the survival curve of WT mice (1100 rads) transplanted with WT (blue curve, n=21) or CFTR$^{\Delta F508}$ (red curve, n=6) BM. (**B**) Typical H&E staining images of intestines from WT mice transplanted with CFTR$^{\Delta F508}$ or WT BM. (**C**-**D**) Quantification of crypts (C, Mean±SD of n=9) and villi (D, Mean±SD of n=27) height of intestines from WT mice transplanted with CFTR$^{\Delta F508}$ or WT BM. n=9. (**E**) Percentage of intestine crypts that contain mucus in it. WT mice are transplanted with WT or CFTR$^{\Delta F508}$ BM. Mean±SD of n=27. n.s. p>0.05, *p<0.05,

***p<0.001 in the Gehan-Breslow-Wilcoxon test (A) and student t-test (C-E). Scale bars are 100 μm.

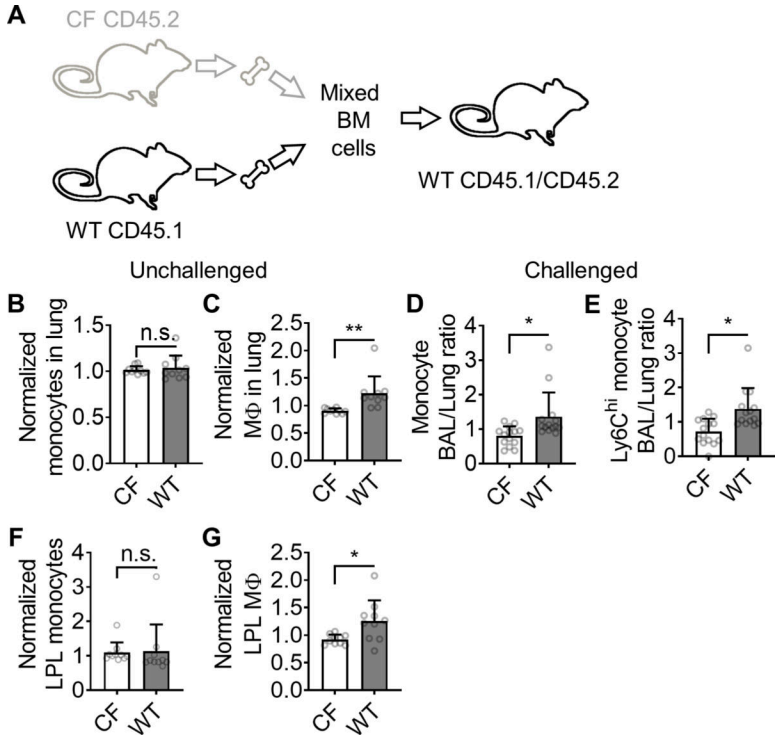

FIGURE 4.

Monocyte recruitment in mixed bone marrow chimeras. (**A**) Schematic showing the establishment of $CFTR^{\Delta F508}$/WT mixed bone marrow chimeras. (**B**-**C**) $CFTR^{\Delta F508}$ and WT monocytes ($CD115^{+}CD11b^{+}CD11c^{-}F4/80^{-}$, B) and macrophages ($F4/80^{+}CD11b^{+}$, C) in the lungs of unchallenged mixed chimeric mice as assessed by flow cytometry. (**D**-**E**) Mixed chimeric mice were challenged with CCL2 (intranasal 100 ng/mice, 12 hours before the harvest) and the BAL/lung monocyte ratio (D) or $Ly6C^{hi}$ BAL/lung monocyte ratio (E) was calculated for $CFTR^{\Delta F508}$ and WT monocytes. (**F**-**G**) The small intestinal lamina propria leukocytes (LPL) of mixed chimeric mice were harvested assessed for monocytes ($CD11b^{+}CD11c^{-}F4/80^{-}Ly6G^{-}TCR^{-}Cd19^{-}NK1.1^{-}$, F) and macrophages ($F4/80^{+}$, G) by flow cytometry. Mean±SD of n=10 mice for B-C, F-G and 14 mice for D-E. n.s. $p>0.05$, *$p<0.05$, **$p<0.01$ in the student T-test.

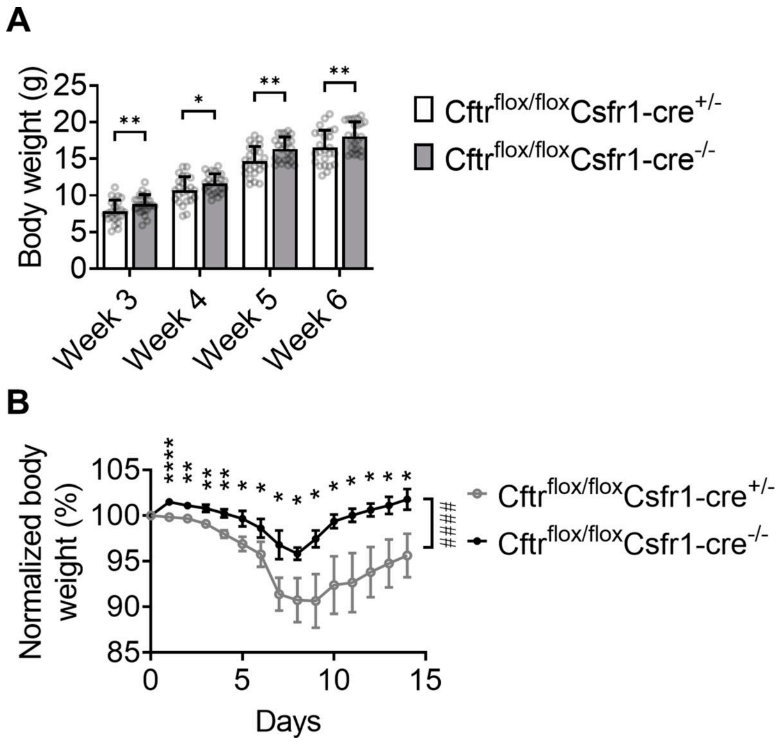

FIGURE 5.

Monocyte-specific CFTR deficiency retards weight gains and exacerbates DSS-induced colitis in mice. (**A**) Body weights of Cftr$^{flox/flox}$Csfr1-cre$^{+/-}$ and Cftr$^{flox/flox}$Csfr1-cre$^{-/-}$ littermates at indicated ages. Mean±SD of n=24 Cftr$^{flox/flox}$Csfr1-cre$^{+/-}$ and 25 Cftr$^{flox/flox}$Csfr1-cre$^{-/-}$ mice. (**B**) Body weights of Cftr$^{flox/flox}$Csfr1-cre$^{+/-}$ and Cftr$^{flox/flox}$Csfr1-cre$^{-/-}$ littermates at indicated days after DSS-induced colitis. Mean±SD of n=7 mice each. *p<0.05, **p<0.01, ****p<0.0001 in the student T-test. ####p<0.0001 in the 2-way ANOVA test.